J Solid State Electrochem (2006) 10: 360–372
DOI 10.1007/s10008-005-0686-2

ORIGINAL PAPER

Abdel Aziz Jbarah · Rudolf Holze

A comparative spectroelectrochemical study of the redox electrochemistry of nitroanilines

Published online: 12 October 2005

Abstract The oxidative and reductive electrochemistry of the three isomeric nitroanilines has been studied in neutral (0.1 mol L^{-1} $KClO_4$) and acidic (0.1 mol L^{-1} $HClO_4$) aqueous electrolyte solutions by cyclic voltammetry and surface enhanced Raman spectroscopy (SERS). The cyclic voltammograms recorded for *o*- and *p*-nitroanilines with a gold electrode in acidic solution, scanning toward negative potentials, revealed formation of phenylenediamine not observed in neutral solution. Similar behavior of nitroanilines and phenylenediamines was observed on gold and platinum electrodes. An oxygen–gold adsorbate stretching mode was detected between 400 and 430 cm^{-1} in the SER-spectra of the three isomeric nitroanilines in both electrolyte solutions at positive electrode potentials, implying perpendicular adsorption via the nitro group.

Keywords Spectroelectrochemistry · Nitroanilines · Phenylenediamines · Electroreduction

Introduction

During recent years much attention has been paid to electrochemical investigations of monosubstituted benzenes and substituted anilines by both electrochemical and spectroelectrochemical techniques. The reduction and oxidation potentials of a molecule can be derived from cyclic voltammetry, and this may enable calculation of thermodynamically significant values of E_0, if the electrode process is reversible. When the overall electrode process is not reversible other phenomena, in particular chemical reaction, e.g. polymerization or dehydrogenation, may occur in addition to the charge-transfer process. In many investigations of molecular adsorption preceding the charge transfer and the subsequent charge transfer itself electrochemical methods (e.g. cyclic voltammetry, polarography, chronoamperometry) are used together with spectroscopic methods to obtain more information about adsorbate orientation relative to the electrode surface.

p-Nitroaniline as a particularly prominent member of the family of isomeric nitroanilines has attracted attention because of the specific effects of an electron-withdrawing nitro group and an electron-donating amino group being in the *para* position of an aromatic ring system [1]. This results in low-energy electronic transitions with charge migration within the molecule [2] and greater nonlinear susceptibility [3, 4, 5] making this molecule interesting as material for nonlinear optics [6, 7, 8, 9, 10]. Its use as an end-group in thiol-based self-assembled monolayers has been reported [11]. Pre-resonance and resonance Raman spectra for nitroanilines have been investigated [12, 13].

Phenylenediamines, which are of considerable practical interest because of their use in various technological applications, can be prepared by reduction by chemical and electrochemical routes from the corresponding nitroanilines. Consequently, all the nitroanilines have attracted interest.

The adsorption of *p*-nitroaniline on a platinum electrode has been studied with modulation reflectance spectroscopy [14] (MRS, a variation of electroreflectance spectroscopy, see also [15]) and the adsorption of monosubstituted benzenes at a gold electrode has been studied using surface-enhanced Raman spectroscopy (SERS) [16, 17]. SERS with these molecules has attracted great attention in a variety of research fields, for example surface science, analytical chemistry [18, 19, 20, 21], and nanotechnology.

We selected *o*-, *m*-, and *p*-nitroanilines (*o*-NA, *m*-NA, *p*-NA) as suitable molecular systems for a comparative

A. A. Jbarah · R. Holze (✉)
Technische Universität Chemnitz, Institut für Chemie,
AG Elektrochemie, 09107 Chemnitz, Germany
E-mail: rudolf.holze@chemie.tu-chemnitz.de

study of electrosorption behavior, because they have at least three different anchoring sites (the nitro, the amino function, and the aromatic ring system). In addition these results shall serve as a point of reference for studies of the spectroelectrochemistry of nitroaniline-substituted polyvinylamines [22].

In this study electrochemical measurements were performed under conditions selected as being particular suitable for in-situ spectroscopy with surface-enhanced Raman spectroscopy SERS, they served as a basis for selection of experimental conditions. Relevant results of previously published extensive investigations of the electrochemistry of these compounds are quoted below. Cyclic voltammograms (CV) were recorded for *o*-NA, *m*-NA, and *p*-NA and their respective amino compounds *o*-, *m*-, and *p*-phenylenediamine (*o*-PDA, *m*-PDA, *p*-PDA) in neutral ($KClO_4$) and acidic ($HClO_4$) aqueous electrolyte solutions at gold and platinum electrodes. The CV of phenylenediamine was recorded to aid interpretation of the reduction process of nitroanilines in terms of products and intermediates. The electrolyte was chosen because of the rather weak adsorption of the perchlorate anion compared with most organic molecules. An early polarographic study suggested that *ortho* and *para*-substituted aromatic nitro compounds were reduced to the corresponding amines via a six-electron process [23], whereas more recently *o*-NA and *m*-NA were reduced to the respective PDA in acidic solution at Ti/ceramic TiO_2 electrodes [24]. Similar results were reported for *m*-NA and *p*-NA reduced at a copper electrode [25] and for *m*-NA in the presence of the Ti^{3+}/Ti^{4+} redox system [26]. SERS data of *o*-NA, *m*-NA, and *p*-NA adsorbed on a gold electrode in neutral and acidic perchlorate electrolyte solutions at different electrode potentials are reported; additional information obtained from UV–visible spectroscopy as far as was necessary to interpret the SER spectra is included.

Experimental

Cyclic voltammograms were recorded with gold and platinum sheet working electrodes using neutral (0.1 mol L^{-1} $KClO_4$, pH = 4.90, unbuffered) and acidic (0.1 mol L^{-1} $HClO_4$, pH = 1.2) aqueous solutions as supporting electrolyte and a custom built potentiostat interfaced with a standard PC via an ADDA-converter card operated with custom-developed software. A saturated calomel electrode and a gold or platinum sheet were used as reference and counter electrodes, respectively, in H-cell compartments separated by glass frits. All potentials are quoted relative to the saturated calomel electrode (E_{SCE}).

UV–visible spectra of solutions were recorded with 1 mm cuvets on a Shimadzu UV-2101PC spectrometer.

Raman spectra were recorded on a ISA T64000 spectrometer connected to a Spectraview 2D CCD detection system. Normal Raman spectra of solid nitroanilines (capillary sampling technique) and SER spectra were recorded using 488 nm and 647.1 nm exciting laser light provided by Coherent Innova 70 Series ion lasers, the laser power was measured at the laser head with a Coherent 200 power meter.

Roughening of the gold electrode (polycrystalline 99.99%, polished down to 0.3 μm Al_2O_3), used to confer SERS activity, was performed in a separate cell with an aqueous solution of 0.1 mol L^{-1} KCl by cycling the electrode potential between $E_{SCE} = -800$ mV and $E_{SCE} = 1650$ mV for approximately 10 min [27].

Electrolyte solutions were prepared from 18 MOhm water (Seralpur Pro 90 c), *o*-, *m*-, and *p*-nitroaniline (Fluka), perchloric acid (Acros) and potassium perchlorate (Merck, G.R.) were used as received. Recrystallization of *m*-phenylenediamine (Aldrich, 99 + %), *o*-phenylenediamine, and *p*-phenylenediamine (Merck, p.A.) from diethyl ether was performed under a nitrogen atmosphere The concentration of the supporting electrolytes was 0.1 mol L^{-1}. Saturated solutions of the nitroanilines (approximately 4 mmol L^{-1} *p*-NA, 8 mmol L^{-1} *o*-NA, 6.5 mmol L^{-1} *m*-NA) were used in all electrochemical and SERS experiments. For recording CV of phenylenediamines 2.7 mmol L^{-1} solution was used. All solutions were freshly prepared, purged with nitrogen (99.999%), and all experiments were performed at room temperature (20°C).

Results and discussion

Cyclic voltammograms recorded with a gold electrode in a 0.1 mol L^{-1} $HClO_4$ electrolyte solution saturated with *p*-NA scanned toward negative potentials starting at $E_{SCE} = +700$ mV show a wave at $E_{c,SCE} = -126$ mV, which is caused by reduction of the *p*-nitro-group (Fig. 1a). A redox wave with $E_{a,SCE} = +536$ mV and $E_{c,SCE} = +436$ mV is observed in the second and subsequent cycles. Assignment of this redox wave to reversible oxidation of the amino-group of *p*-NA, as mentioned in previous work [28], is unlikely; the oxidation potential of the *p*-NA amino-group was observed at much higher electrode potentials as discussed below. Actually the redox wave observed in the second cycle of the reduction of *p*-NA corresponds to reversible oxidation of amino groups of the *p*-PDA. This conclusion is based on comparison of this redox wave after *p*-NA reduction with the redox wave obtained when scanning toward positive potentials with *p*-PDA (Fig. 1b). Formation of *p*-PDA by electrochemical reduction of *p*-NA has been discussed in detail in previous work in which reverse-pulse polarography was used [29], and the six-electron reduction process was described in terms of the following ECE (electron transfer, chemical reaction, electron transfer) mechanism [30, 31, 32, 33, 34].

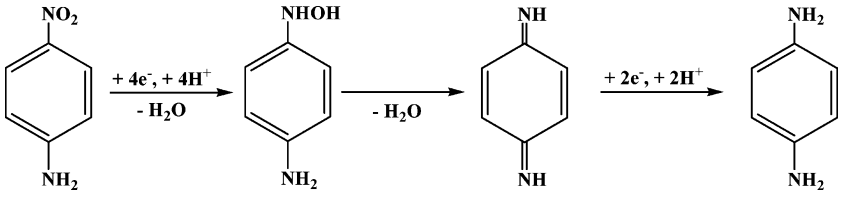

The first reaction intermediate, the radical anion (not shown in this scheme), has frequently been reported on the basis of electron spin resonance spectroscopy [35, 36].

According to this ECE mechanism, formation of *o*-PDA was also observed as a product of the electrochemical reduction of *o*-NA under the same conditions as used for *p*-NA. The cathodic wave observed with *o*-NA at $E_{c,SCE} = -342$ mV corresponds to an anodic wave at $E_{a,SCE} = +546$ mV in the return scan and the second cycle (Fig. 1c); no reduction wave is observed in this scan. The same shape and position of this anodic wave is obtained when scanning *o*-PDA toward positive potentials (Fig. 1d). Obviously the electrooxidation products formed from the electrochemically generated *o*-PDA when scanning toward positive potentials are consumed very rapidly by a nonelectrochemical reaction; according to results discussed below electropolymerization may occur.

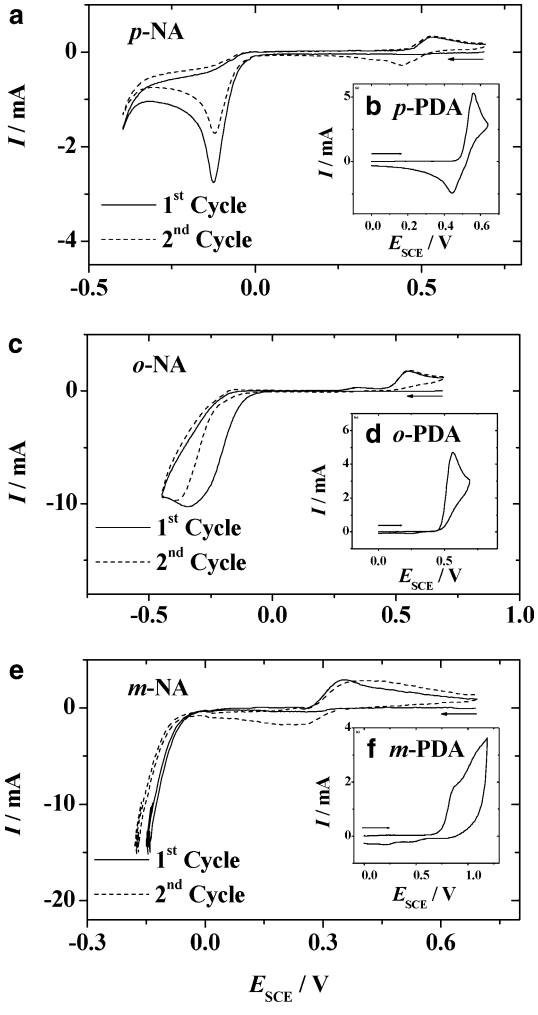

Fig. 1 Cyclic voltammograms obtained with a gold-sheet electrode in a solution of 0.1 mol L^{-1} $HClO_4$ saturated with nitroanilines (scanning toward negative potentials) and 2.7 mmol L^{-1} concentration of phenylenediamines (scanning toward positive potentials); $dE/dt = 0.1$ V s^{-1}, room temperature, nitrogen purged

In contrast with our observations with both *o*-NA and *p*-NA, obviously no *m*-PDA as a product of electrochemical reduction of *m*-NA is formed when scanning toward negative potentials limited only by hydrogen evolution (Fig. 1e), on the basis of comparison with the behavior of *m*-PDA (Fig. 1f). However, some reduction of product of *m*-NA causing a redox wave with $E_{a,SCE} = +351$ mV and $E_{c,SCE} = +222$ mV observed in the backward scan and subsequent potential cycles must have been formed (Fig. 1e). This redox wave is significantly different from the poorly defined anodic wave observed at $E_{a,SCE} = +870$ mV for electrooxidation of *m*-PDA when scanning toward positive potentials (Fig. 1f).

Early polarographic studies of nitroanilines in absolute ethanol and in ethanol–water and tetrahydrofuran–water mixtures [37, 38, 39] suggested, that *o*-NA and *p*-NA underwent six-electron reduction processes whereas *m*-NA gave four-electron waves only at low pH [40]. In later studies of reduction of the isomers complicated ECE mechanisms have been reported [41] and the substantial effect of the electrolyte solution, including pH, has been pointed out [42, 43]. Furthermore, for *o*-NA and *p*-NA the possibility of formation of quinone-like species would facilitate reduction to the respective amine whereas for *m*-NA the reduction might yield intermediates subject to subsequent rearrangement and condensation.

In scans toward negative potentials of solutions saturated with nitroanilines in acidic electrolyte all the CV recorded with a platinum electrode showed only hydrogen evolution.

Special behavior of *m*-NA was also observed in CV recorded with a gold electrode when scanning toward positive potentials, starting at $E_{SCE} = 0$ mV, in acidic electrolyte solution. Oxidation of the amino group causes an anodic wave at $E_{a,SCE} = +1045$ mV, substantially lower than the anodic waves obtained with *p*-NA at $E_{a,SCE} = +1123$ mV and with *o*-NA at $E_{a,SCE} = +1150$ mV (Fig. 2a). The same order of

oxidation waves of the nitroanilines with approximately the same positions was observed when using a platinum electrode (Fig. 2b); this is in perfect agreement with the order previously observed with a platinum electrode in an acetonitrile-based nonaqueous electrolyte solution [44]. It is evident that the radical intermediate formed during electrochemical oxidation of the amino group of aniline is destabilized when the strong electron-withdrawing NO_2 group is located in the *ortho* or *para* positions, as illustrated in the following resonance structures of the aniline radical cation [45].

In electrooxidation of the isomeric phenylenediamines at a gold electrode the CV of *p*-PDA implies stability of the oxidized species at least sufficient to enable detection of the corresponding current wave assigned to reduction of this intermediate (Fig. 1b), this reduction current is not observed for *o*-PDA (Fig. 1d) and *m*-PDA (Fig. 1f). It is known from previous work that polymerization of *m*-PDA and *o*-PDA occurs during electrochemical oxidation [46, 47, 48, 49]. For *p*-PDA this polymerization is inhibited by the blocking of the *para* position of the benzene ring, which is, in most

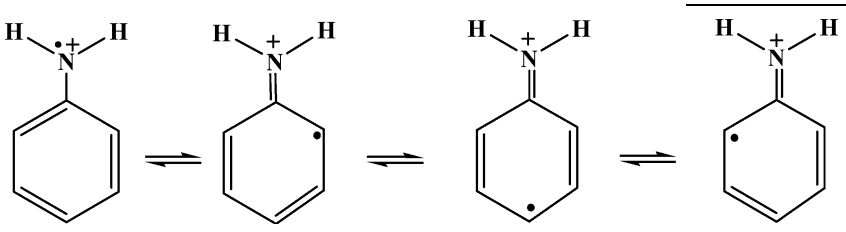

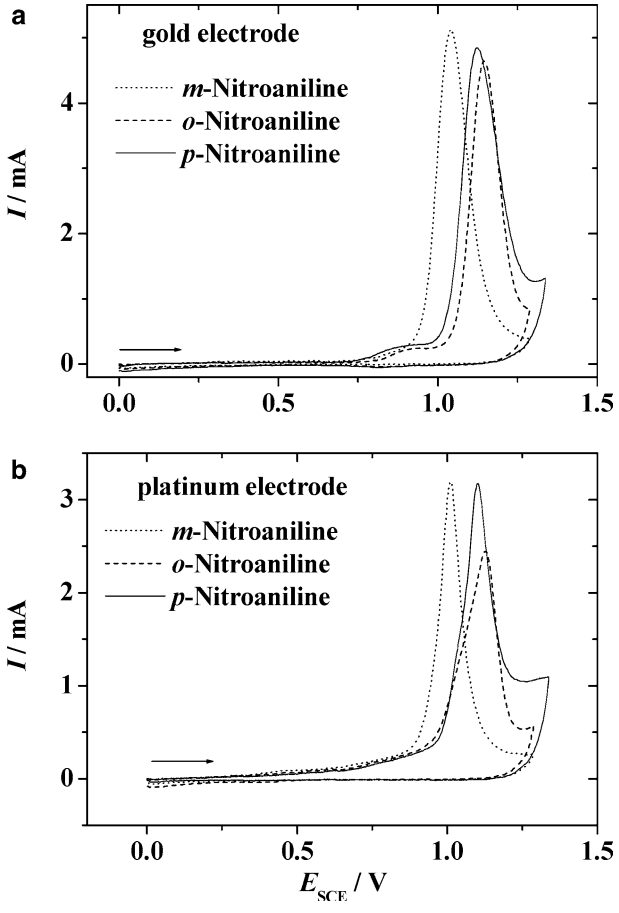

Fig. 2 Cyclic voltammograms obtained from gold and platinum-sheet electrodes in a solution of 0.1 mol L^{-1} $HClO_4$ saturated with nitroanilines, scanning toward positive potentials; $dE/dt = 0.1$ V s^{-1}, room temperature, nitrogen purged

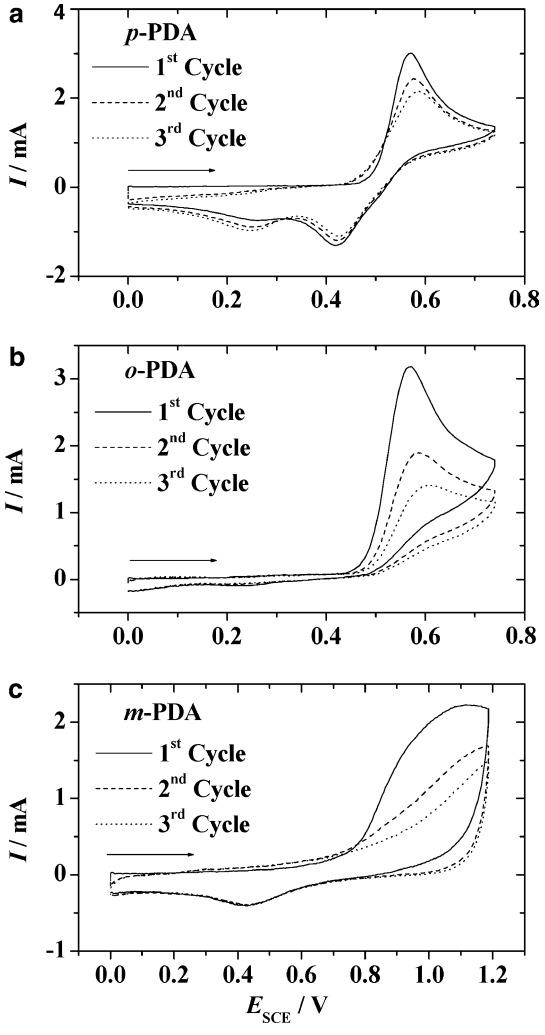

Fig. 3 Cyclic voltammograms obtained from a platinum-sheet electrode in a solution of 0.1 mol L^{-1} $HClO_4$ containing 2.7 mmol L^{-1} phenylenediamines, scanning toward positive potentials; $dE/dt = 0.1$ V s^{-1}, room temperature, nitrogen purged

polyanilines, the preferred coupling position. The same features were observed for phenylenediamines in CV with a platinum electrode in acidic electrolyte solution (Fig. 3). The slow growth of the cathodic wave at $E_{c,SCE} = +251$ mV assigned to reduction of an electrochemically redox-active polymer was observed clearly in the second and third cycles of CV with *p*-PDA combined with the slowly disappearing redox waves ($E_{a,SCE} = +570$ mV, $E_{c,SCE} = +420$ mV) corresponding to oxidation of monomeric *p*-PDA and reduction of the reaction intermediate (presumably the radical cation) (Fig. 3a). The cathodic signal of the growing polymer formed electrochemically was not discussed further in earlier investigations [50, 51, 52, 53, 54]. The CVs recorded for *m*-PDA and *o*-PDA at a platinum electrode reveal polymerization is faster than for *p*-PDA. The poorly defined anodic wave assigned to oxidation of *m*-PDA disappeared in the second and third cycle, indicating inhibition of further monomer oxidation, whereas the cathodic wave at $E_{c,SCE} = +426$ mV indicated redox activity of the formed polymer (Fig. 3c). A similar rapid decrease, but not disappearance, of the oxidation wave was observed for *o*-PDA (Fig. 3b). In this case no significant redox activity of a conceivable polymer was observed.

In neutral unbuffered electrolyte solution (0.1 mol L^{-1} $KClO_4$) results for all the nitroanilines, at both gold and platinum electrodes, were different from those obtained in scans toward negative potentials in acidic electrolyte solutions. The cathodic waves observed for nitroaniline reduction (*p*-NA at $E_{c,SCE} = -821$ mV (Fig. 4a), *o*-NA at $E_{c,SCE} = -766$ mV (Fig. 4c), *m*-NA at $E_{c,SCE} = -764$ mV (Fig. 4e)) at a gold electrode are associated with two poorly defined anodic waves and one cathodic wave for *p*-NA ($E_{a1,SCE} = -100$ mV, $E_{a2,SCE} = -10$ mV, $E_{c,SCE} = -173$ mV) and *o*-NA ($E_{a1,SCE} = +30$ mV, $E_{a2,SCE} = +195$ mV, $E_{c,SCE} = -88$ mV), and a redox wave for *m*-NA ($E_{a,SCE} = -288$ mV, $E_{c,SCE} = -358$ mV).

Previous investigations of *p*-NA with normal and reverse-pulse polarography at high pH suggested three electroactive products of *p*-NA reduction [29]. The authors suggested that the two anodic waves reflect the oxidation of *p*-amino-*N*-phenylhydroxylamine and *p*-PDA and the cathodic wave corresponds to reduction of *p*-nitroaniline which is formed during a homogeneous reaction as follows:

Our results imply the formation of *p*-amino-*N*-phenylhydroxylamine, which is oxidized when scanning toward positive potentials, and *p*-nitroaniline, which is subsequently reduced. Formation of *p*-PDA is unlikely because its oxidation was observed at higher potentials only (see CV recorded under the same con-

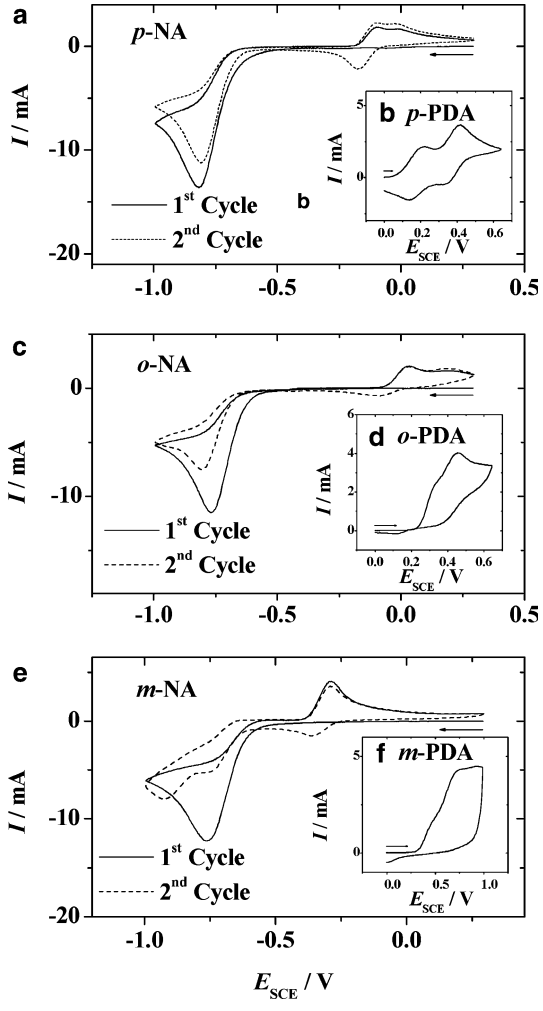

Fig. 4 Cyclic voltammograms obtained from a gold-sheet electrode in a solution of 0.1 mol L^{-1} $KClO_4$ saturated with nitroanilines (scanning toward negative potentials starting at $E_{SCE} = 0.3$ V) and 2.7 mmol L^{-1} phenylenediamines (scanning toward positive potentials starting at $E_{SCE} = 0$ V); $dE/dt = 0.1$ V s^{-1}, room temperature, nitrogen purged

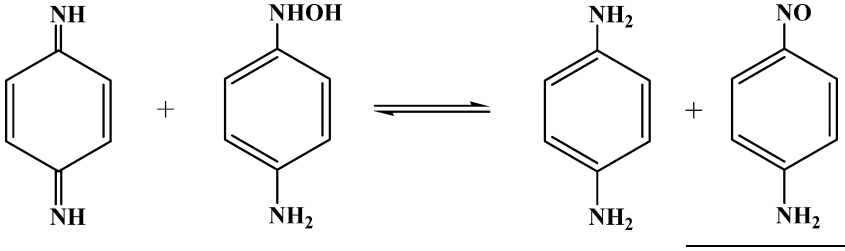

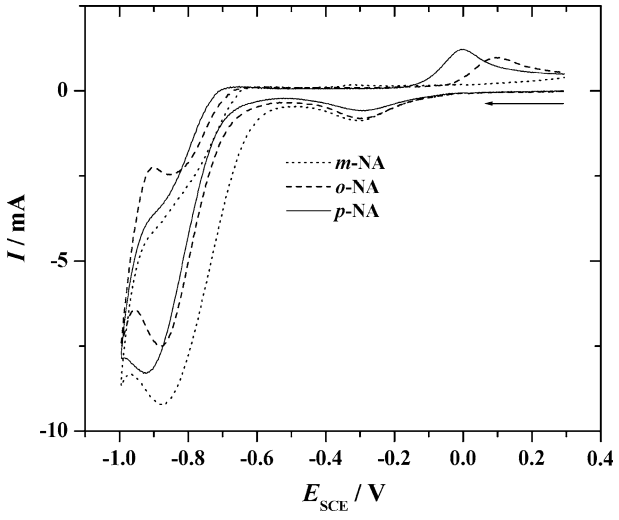

Fig. 5 Cyclic voltammograms obtained from a platinum-sheet electrode in 0.1 mol L^{-1} $KClO_4$ saturated with nitroanilines, scanning toward negative potentials starting at $E_{SCE} = 0.3$ V; $dE/dt = 0.1$ V s^{-1}, room temperature, nitrogen purged

ditions (Fig. 4b)). Assignment of the poorly resolved double peak in the anodic scan to two different reduction intermediates or further products is currently impossible. Stočesová, on the other hand, proved that in acidic medium nitrobenzene is reduced to aniline via a phenylhydroxylamine intermediate whereas in alkaline medium (pH≥5) phenylhydroxylamine is the final product and no further reduction occurs [55].

m-NA is reduced more easily (at less negative potentials) than both *o*-NA and *p*-NA. This reflects the position effect of the substituent. Substituents increasing the electron density at the nitro group make the reduction more difficult, as is observed for *o*-NA and *p*-NA, whereas the opposite is true for *m*-NA in which the nitro group is in a position which reduces the electron density at the nitro group, as discussed in detail in a previous study [37]. The same order of reduction potentials was also observed in CV recorded with a

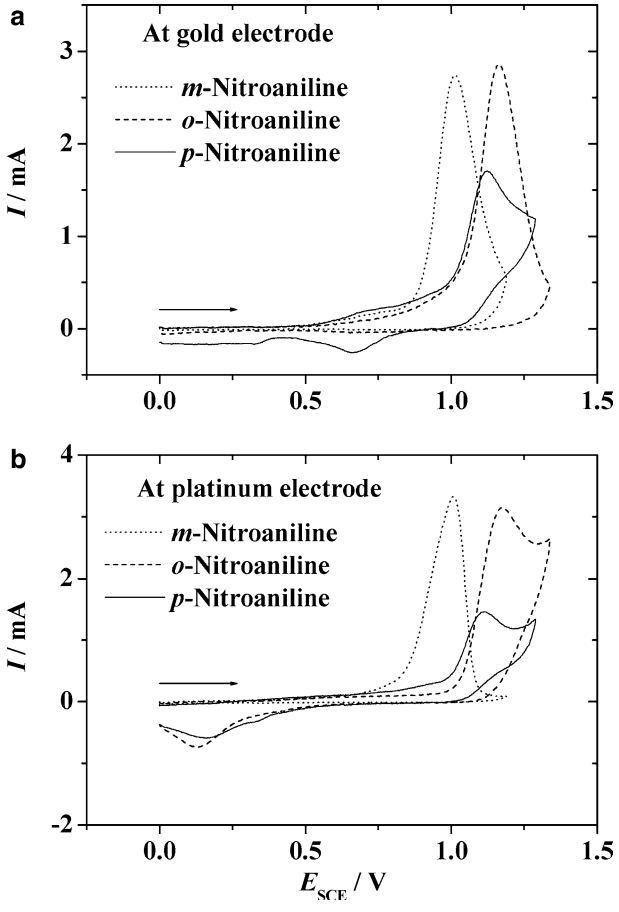

Fig. 6 Cyclic voltammograms obtained from gold and platinum-sheet electrodes in 0.1 mol L^{-1} $KClO_4$ saturated with nitroanilines, scanning toward positive potentials; $dE/dt = 0.1$ V s^{-1}, room temperature, nitrogen purged

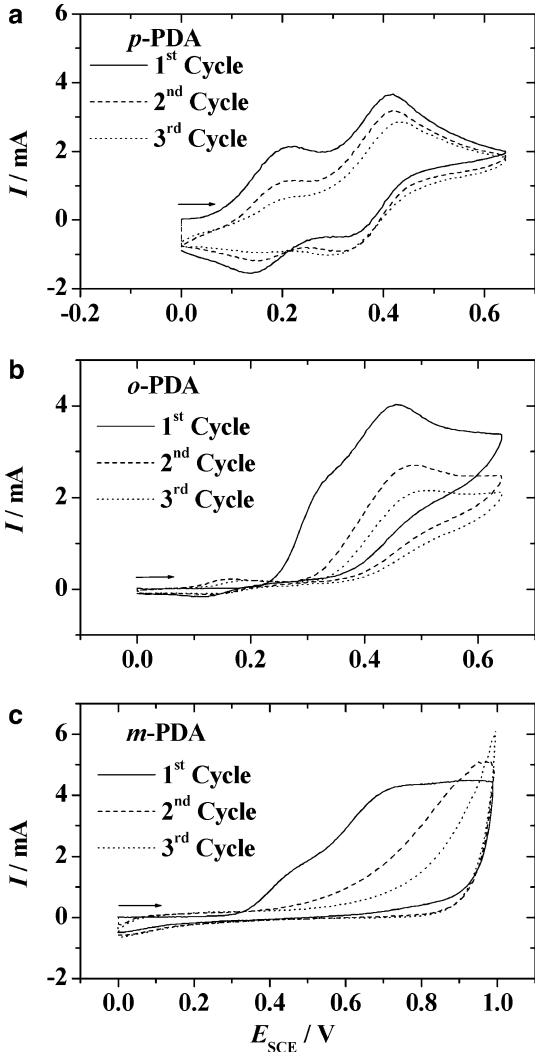

Fig. 7 Cyclic voltammograms obtained from a platinum-sheet electrode in 0.1 mol L^{-1} $KClO_4$ containing 2.7 mmol L^{-1} phenylenediamines, scanning toward positive potentials starting at $E_{SCE} = 0$ V; $dE/dt = 0.1$ V s^{-1}, room temperature, nitrogen purged

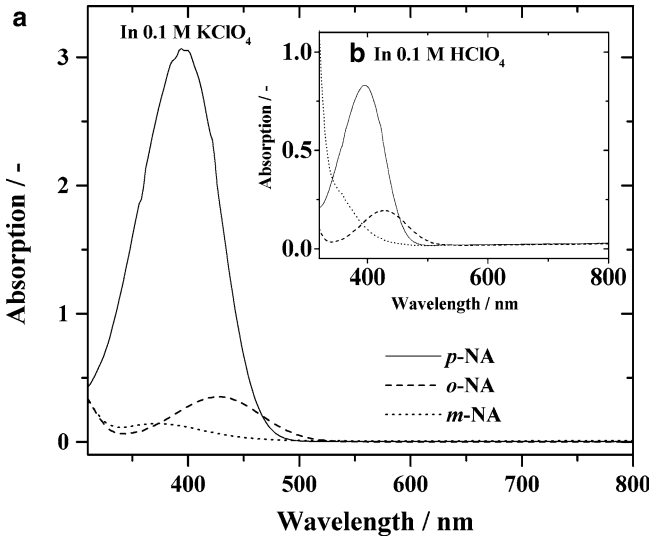

Fig. 8 UV–visible spectra obtained from saturated with aqueous solutions of nitroanilines in (**a**) 0.1 mol L^{-1} $KClO_4$ and (**b**) 0.1 mol L^{-1} $HClO_4$; 1-mm cell

platinum electrode in the neutral electrolyte solution (*p*-NA at $E_{c,SCE} = -923$ mV, *o*-NA at $E_{c,SCE} = -882$ mV, *m*-NA at $E_{c,SCE} = -875$ mV, Fig. 5).

In a scan toward positive potentials starting at $E_{SCE} = 0$ mV in neutral electrolyte solution saturated with nitroaniline the CV recorded with gold show waves at $E_{a,SCE} = +1164$ mV, $E_{a,SCE} = +1013$ mV, and $E_{a,SCE} = +1120$ mV for *o*-NA, *m*-NA, and *p*-NA respectively (Fig. 6a), nearly the same positions as these waves observed with a platinum electrode under the same conditions (Fig. 6b). The close agreement of the sequence of these waves with those obtained and discussed with an acidic electrolyte is obvious. The CV obtained from *p*-NA with both electrodes also contain a poorly defined cathodic wave at $E_{c,SCE} = +1054$ mV. It is usually assumed that the radical cation formed during electrochemical oxidation of aniline and substituted anilines [56, 57] undergoes rapid head-to-tail coupling [58, 59, 60]. Copolymers of aniline and nitroaniline have been prepared chemically [60]. For the *p*-NA isomer it was initially suggested that this coupling was obstructed

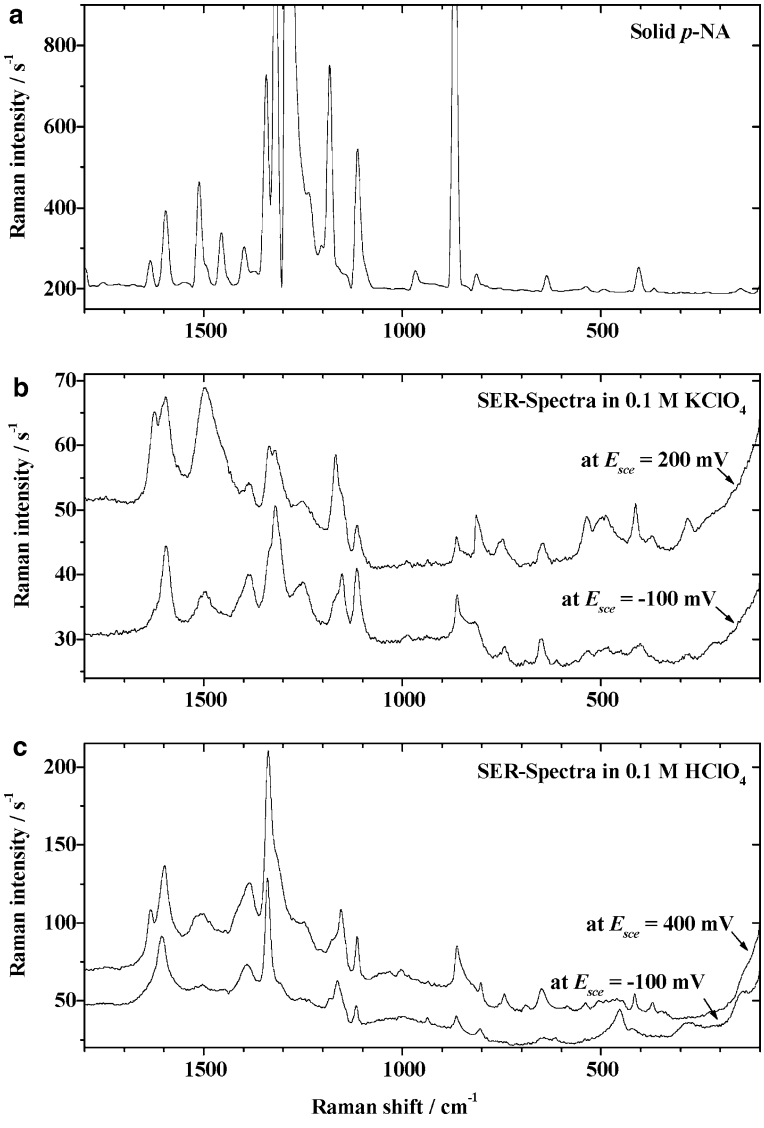

Fig. 9 (**a**) Normal Raman spectrum of solid *p*-NA, capillary sampling technique, 488 nm laser light; (**b**) and (**c**) SER spectra of *p*-NA adsorbed on a gold electrode at the electrode potentials indicated in neutral and acidic perchlorate solution, respectively, 647.1 nm

Table 1 Spectral data for *p*-nitroaniline (*p*-NA) as a solid and adsorbed on a gold electrode at different electrode potentials and in different electrolyte solutions

Mode	Wilson mode #	*p*-NA solid (Fig. 9a)	0.1 mol $L^{-1}KClO_4$ (Fig. 9b)		0.1 mol $L^{-1}HClO_4$ (Fig. 9c)	
			$E_{SCE} = 200$ mV	$E_{SCE} = -100$ mV	$E_{SCE} = 400$ mV	$E_{SCE} = -100$ mV
C-N-torsion	–	149	–	–	–	144
n.a.	–	–	284	284	–	283
δ(ring)	6a	365	371	–	368	–
γ(ring)	16a	404	–	400	–	–
$\nu_{Au\text{-}O}$	–	–	411	–	415	–
n.a.	–	–	–	451	–	451
γ(ring)	16b	492	493	494	–	–
$\beta_{as}(NO_2)$	–	536	528	534	532	–
δ(ring)	6b	634	649	647	646	646
$\gamma_s NO_2$	–	–	750	740	743	–
γ(CH)	10a	811	811	818	800	805
$\beta_s NO_2$	–	865	861	863	857	864
γ(CH)	17a	965	–	–	–	–
δ(CH)	18b	1110	1114	1111	1112	1113
δ(CH)	9a	1181	1168	1151	1153	1159
δ(CH)	3	1277	1252	1251	1250	1251
ν(ring)	14	1317	1316	1315	–	–
$\nu_s NO_2$	–	1339	1334	–	1335	1337
νC-NH_2	–	1396	1385	1383	1383	1391
ν(ring)	19b	1453	–	–	–	–
ν(ring)	19a	1508	1497	1496	1501	1497
ν(ring)	8a	1595	1594	1595	1598	1607
$\beta_s NH_2$	–	1632	1626	–	1634	–

δ, in-plane deformation; γ, out-of-plane deformation; ν, stretching; ν_s, symmetric stretching; β_{as}, rocking; γ_s, wagging; β_s, scissoring

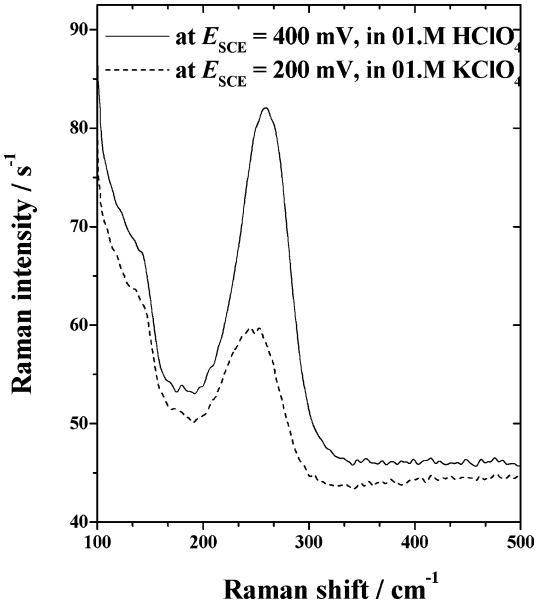

Fig. 10 SER spectra of adsorbed perchlorate anions on a gold electrode, 647.1 nm

by the presence of the nitro group in the *para* position; a study of the respective polymers prepared by chemical polymerization showed this to be incorrect [59]. Nevertheless the, presumably, slower subsequent polymerization leaves some radical cations available for electroreduction.

Polymerization of phenylenediamines during electrochemical oxidation at gold and platinum electrodes was also observed in neutral electrolyte. The anodic wave obtained with *o*-PDA at $E_{a,SCE} = +454$ mV (Fig. 7b) and the poorly defined wave obtained with *m*-PDA at $E_{a,SCE} = +750$ mV (Fig. 7c) disappeared rapidly during the second and third cycles, implying the formation of a product on the electrode surface inhibiting further electrooxidation. For *p*-PDA the amplitude of the current of the two anodic waves at $E_{a1,SCE} = +212$ mV and $E_{a2,SCE} = +413$ mV and the cathodic wave at $E_{c1,SCE} = +139$ mV decreased only slowly; at the same time another cathodic wave at $E_{c2,SCE} = +340$ mV (Fig. 7a) appeared. It is highly probable the growing cathodic wave corresponds to the polymer slowly growing on the electrode surface as discussed for the acidic solution; the other three waves correspond to redox processes of *p*-PDA.

We recorded UV–Vis spectra of saturated nitroanilines in 0.1 mol L^{-1} $KClO_4$ and $HClO_4$, a set of spectra is shown in Fig. 8. The major band attributed to the $\pi \rightarrow \pi^*$ transition is found at 428 nm, 375 nm, and 395 nm for *o*-NA, *m*-NA, and *p*-NA, respectively, for aqueous solutions in 0.1 mol L^{-1} $KClO_4$. In $HClO_4$ these bands were observed for *o*-NA and *p*-NA only—for *m*-NA the band is very poor, possibly because of a protonation effect. Because the excitation wavelength of 647.1 nm used in SERS measurements is far from absorption bands for all nitroanilines SERS spectra were measured under off-resonance conditions.

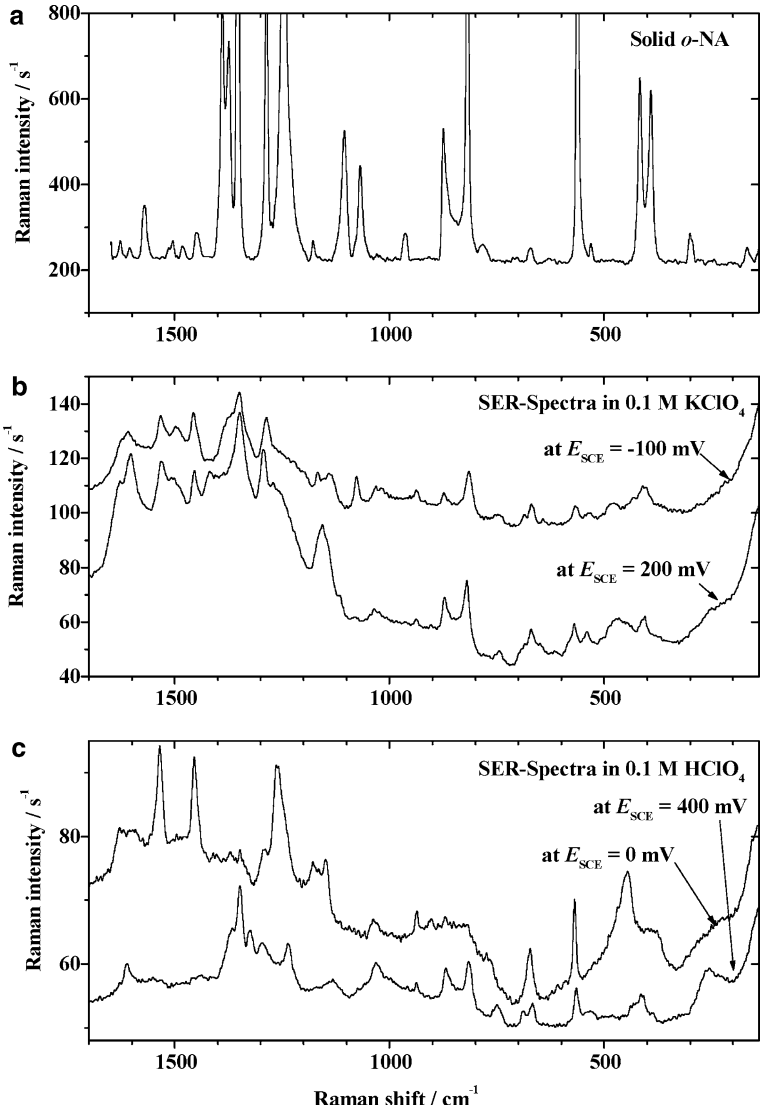

Fig. 11 (**a**) Normal Raman spectrum of solid *o*-NA, capillary sampling technique, 647.1 laser light; (**b**) and (**c**) SER spectra of *o*-NA adsorbed on a gold electrode at the electrode potentials indicated in neutral and acidic perchlorate solution, respectively, 647.1 nm

Band positions from a Raman spectrum of solid *p*-NA (Fig. 9a) and from SER-spectra of *p*-NA adsorbed from neutral (Fig. 9b) and acidic (Fig. 9c) electrolyte solutions are listed in Table 1; assignment of the observed lines is based on literature data [28, 61, 62, 63]. The SER-spectra of *p*-NA and its isomers were initially recorded only within a potential window between oxidation and reduction potentials to avoid contributions from reduction/oxidation products. In the SER spectrum of adsorbed *p*-NA intensities of several in-plane modes were increased relative to those of the out-of-plane modes in both electrolyte solutions over the whole range of electrode potentials investigated. This implies perpendicular orientation of the adsorbed molecule; a similar conclusion has been reported for, e.g., benzene and selected monosubstituted benzenes adsorbed on gold [64]. This orientation has also been deduced from limited experimental studies combined with DFT calculations for *p*-NA adsorbed on silver colloids [65] and from SER-studies with a silver electrode [66].

In the low-wave-number region an additional band not seen with solid *p*-NA is found at 411 and 415 cm^{-1} in neutral and acidic electrolyte solutions, respectively. This mode cannot be caused by the gold–oxygen mode of the adsorbed perchlorate, which was found at approximately 270 cm^{-1} in a previous study [27] and at 262 and 251 cm^{-1} in acidic and neutral electrolytes, respectively, in this study (Fig. 10). Thus this band must be caused by interaction between the adsorbed *p*-NA and the gold surface. A variety of modes of interaction between adsorbed *p*-nitroaniline and the electrode surface are conceivable and may involve the aromatic electron system of benzene ring, hydrogen atoms on the ring, or substituent groups. Perpendicular orientation of adsorbed *p*-NA as mentioned above, and the coordinating capability of the substituent, makes interaction with the electrode surface via the oxygen atoms of the nitro group or the free electron pair of the amino group likely. It has been reported that the gold–oxygen stretching mode occurs in the range 400 to 500 cm^{-1} (e.g. approximately 412 cm^{-1} in Ref. [28]), whereas the

Table 2 Spectral data for *o*-nitroaniline (*o*-NA) as a solid and adsorbed on a gold electrode at different electrode potentials and in different electrolyte solutions

Mode	Wilson mode #	*o*-NA solid (Fig. 11a)	0.1 mol $L^{-1}KClO_4$ (Fig. 11b)		0.1 mol $L^{-1}HClO_4$ (Fig. 11c)	
			$E_{SCE} = 200$ mV	$E_{SCE} = -100$ mV	$E_{SCE} = 400$ mV	$E_{SCE} = 0$ mV
n.a.	–	167	–	–	–	–
n.a.	–	298	–	–	262	–
n.a.	–	392	–	–	–	–
$\nu_{Au\text{-}O}$	–	–	406	404	410	–
γ(ring)	16b	419	–	–	–	–
n.a.	–	–	–	–	–	445
n.a.	–	–	472	478	–	–
$\beta_{as}(NO_2)$	–	530	537	531	531	–
δ(ring)	6a	560	569	564	561	569
ν(ring)	1	670	668	667	662	670
γ(CH)	11	780	744	744	747	–
δ(ring)	12	817	821	816	816	–
γ(CH)	17a	872	867	870	865	–
γ(CH)	5	961	938	936	936	934
δ(CH)	18b	–	1031	1023	1027	1031
$\beta_{as}NH_2$	–	1067	1076	1076	–	–
ν(CH)	13	1100	–	–	–	–
δ(CH)	9b	–	1148	1137	1133	1144
δ(CH)	9a	1176	–	1162	–	1176
ν(CH)	7a	1247	–	–	1231	1262
ν(ring)	14	1288	1287	1283	1295	1290
$\nu_s NO_2$	–	1353	1347	1349	1321	1348
n.a	–	1370	–	–	1365	1369
n.a	–	1388	–	–	–	–
ν(ring)	19a	1446	1453	1455	–	1450
ν(ring)	19b	1478	1494	1493	–	–
$\nu_{as}NO_2$	–	1509	1524	1528	–	1529
ν(ring)	8a	1569	–	–	–	–
ν(ring)	8b	1601	1600	1606	1608	1601 broad
$\beta_s NH_2$	–	1625	1626	–	–	–

δ, in-plane deformation; γ, out-of-plane deformation; ν, stretching; ν_s, symmetric stretching; ν_{as}, asymmetric stretching; β_{as}, rocking; β_s, scissoring

gold–amino nitrogen stretching mode is found at approximately 341 cm^{-1} [67] (on silver it is observed at 215 cm^{-1} [63]). In addition, the broadening and the downshift of the rocking, scissoring, and symmetric stretching modes of nitro group at $E_{SCE} = 400$ and 200 mV in acidic and neutral electrolyte, respectively, support the assumed adsorption via the nitro group. This adsorption mode was not observed at a more negatively charged surface at $E_{SCE} = -100$ mV. This is attributed to electrosorption of the anilinium cation of protonated *p*-NA in both acidic and neutral electrolytes (0.1 mol L^{-1} $KClO_4$, pH = 4.90, unbuffered and only slightly acidic). Electrostatic adsorption of the anilinium cation without any of the functional groups acting as anchors is also evident from the disappearance of the scissoring mode of the amino group on the negatively charged surface. A new strong band in acidic solution and a weak one in neutral solution was, moreover, observed at 451 cm^{-1} for negative surface charge, presumably as a result of electrosorption of the anilinium cation.

Bands observed in a normal Raman spectrum (Fig. 11a) and SER spectra of adsorbed *o*-NA for neutral (Fig. 11b) and acidic (Fig. 11c) electrolyte solutions are listed in Table 2; assignment of the observed lines is based on literature data [61, 62]. As was observed for *p*-NA, the *o*-NA adsorbs in a perpendicular orientation as deduced from the SER spectra, in which the in-plane modes are enhanced compared with the out-of-plane modes, which are relatively weak or absent. In a solution of $KClO_4$ the SER spectra show the oxygen–gold mode at 406 cm^{-1}. Appearance of this mode at lower electrode potentials does not agree with our observations for *p*-NA (vide supra); this might be because the degree of protonation of the amino group of *o*-NA is lower than for *p*-NA. Protonation of *o*-NA is more difficult because of formation of intramolecular hydrogen bonds between one oxygen of the nitro group and the amino group, as reported in a study of the optimized structures of substituted anilines by density function theory (DFT) [68]. This interaction is also reflected in the adsorption behavior of *o*-NA at a gold surface via one oxygen atom only at a lower wavenumber compared with adsorption via two oxygen atoms for *p*-NA. In acidic electrolyte solution the oxygen–gold mode was observed at 410 cm^{-1} at more positive electrode potential ($E_{SCE} = 400$ mV). When we move in the direction of negative potential ($E_{SCE} = -100$ mV) this mode disappeared and was replaced by a new strong mode at 445 cm^{-1}. This might be because of electrosorption of

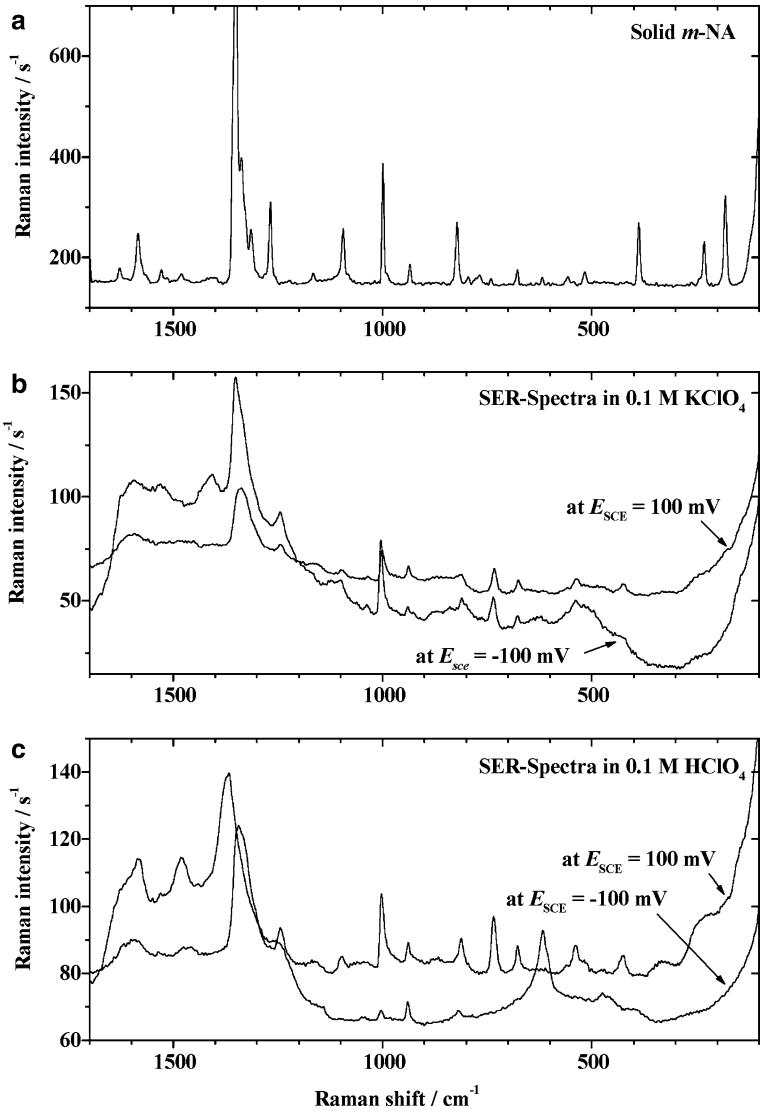

Fig. 12 (**a**) Normal Raman spectrum of solid *m*-NA, capillary sampling technique, 647.1 laser light; (**b**) and (**c**) SER- spectra of *m*-NA adsorbed on a gold electrode at the potentials indicated in neutral and acidic perchlorate solution, respectively, 647.1 nm

the anilinium cation of *o*-NA as discussed above for *p*-NA.

The overall Raman scattering intensities of *m*-NA are weaker than those of *p*-NA and *o*-NA as shown in the normal Raman spectrum of solid *m*-NA and SER spectra of adsorbed *m*-NA (Fig. 12, Table 3) [61, 62, 69]). The nitro group of *m*-NA cannot efficiently accommodate the electron donated by the amino group, which leads to lower electron density of the nitro-group oxygen atoms. This is reflected in the shift of the observed oxygen–gold mode to higher wavenumbers at 423 cm^{-1} in the SER spectra of *m*-NA in neutral electrolyte solution at $E_{SCE} = 100$ mV compared with the position of this mode for *p*-NA and *o*-NA. The existence of this band implies adsorption via the nitro function. Comparison of the position of this band under otherwise the same conditions provides some insight into the effects of molecule–solvent interaction and simultaneous electronic resonance effects. The effect of molecule–solvent interaction [70] in the absence of any resonant charge redistribution results in *m*-NA having the relatively highest negative charge density on the nitro group and—in turn—the strongest interaction with the gold surface, as is evident from the highest wavenumber (423 cm^{-1}). For *p*-NA this effect is much less pronounced, the band is red-shifted to 411 cm^{-1}. With *o*-NA the resonance charge transfer is practically absent; in addition, one oxygen is interacting intramolecularly with a hydrogen of the amino group (presumably only one oxygen instead of two is interacting with the metal) causing a further red-shift to 406 cm^{-1}. At a less positive electrode potential of $E_{SCE} = -100$ mV this band disappeared completely; at the same time the asymmetric stretching mode of NO_2 at 1533 cm^{-1} and also the symmetric stretching of this group appeared and became more intense and sharp. The absence of the oxygen–gold mode and these other changes seem to indicate a mode of adsorption with the nitro function not engaged as an anchoring group. The absence of any other mode indicating an interaction via, e.g., the amino

Table 3 Spectral data for *m*-nitroaniline (*m*-NA) as a solid and adsorbed on a gold electrode at different electrode potentials and in different electrolytes

Mode	Wilson mode #	*m*-NA solid (Fig. 12a)	0.1 mol $L^{-1}KClO_4$ (Fig. 12b)		0.1 mol $L^{-1}HClO_4$ (Fig. 12c)	
			$E_{SCE} = 100$ mV	$E_{SCE} = -100$ mV	$E_{SCE} = 100$ mV	$E_{SCE} = -100$ mV
n.a.	–	178	–	–	–	–
n.a.	–	231	–	–	–	–
δ(ring)	6b	385	–	–	332	–
$\nu_{Au\text{-}O}$	–	–	423	–	424	–
n.a.	–	–	–	–	–	469
δ(ring)	6a	514	532	537	536	–
γ(ring)	16a	555	–	–	–	–
$\gamma_s NH_2$	–	616	–	–	–	612
γ(ring)	4	677	673	673	674	–
$\gamma_s NO_2$	–	739	730	736	729	–
n.a.	–	770	–	–	–	–
γ(CH)	11	791	–	–	–	–
ν(CH)	7b	817	809	809	810	814
γ(CH)	17a	929	935	940	935	936
δ(ring)	12	999	1000	999	1001	1001
δ(CH)	18b	1099	1095	1098	1096	–
δ(CH)	9b	1164	1160	–	1160	–
ν(CH)	13	1269	1243	1243	1242	1250
δ(CH)	3	1309	–	–	–	–
ν(ring)	14	1335	–	–	–	–
$\nu_s NO_2$	–	1350	1350	1341	1344	1363
ν(ring)	19a	1407	–	1407	–	–
ν(ring)	19b	1483	–	–	1464	1478
$\nu_{as} NO_2$	–	1533	–	1533	–	–
ν(ring)	8a	1585	1593	1593	1596	1581
$\beta_s NH_2$	–	1631	–	–	–	–

δ, in-plane deformation; γ, out-of-plane deformation; ν, stretching; ν_s, symmetric stretching; ν_{as}, asymmetric stretching; γ_s, wagging; β_s, scissoring

function leaves this suggestion unsubstantiated at the moment.

In acidic electrolyte solution the oxygen-gold mode at 424 cm^{-1} was observed at positive electrode potentials, it again disappeared at more negative electrode potentials, whereas the wagging mode of NH_2 at 612 cm^{-1} was strongly enhanced. In acidic electrolyte a poorly defined broad band at approximately 469 cm^{-1} was observed for *m*-NA at less positive electrode potentials than observed for *o*-NA and *p*-NA.

Conclusions

The position of substituent groups and the pH of the electrolyte have a substantial effect on oxidation and reduction processes of the nitroanilines and phenylenediamines at surfaces. A variety of adsorption behavior of the three nitroanilines at gold was observed; this clearly depends on the applied electrode potential. The amount of electronic interaction between the amino and nitro groups in the nitroanilines also affects the position of the vibrational bands.

Acknowledgment Financial support from the Fonds der Chemischen Industrie and the Deutsche Forschungsgemeinschaft is gratefully acknowledged.

References

1. Nobutoki H, Koezuka H (1997) J Phys Chem 101:3762
2. Bertinelli F, Palmieri P, Brillante A, Taliani C (1977) Chem Phys 25:333
3. Stähelin M, Burland DM, Rice JE (1992) Chem Phys Lett 191:245
4. Woodford JN, Pauley MA, Wang CH (1997) J Phys Chem A 101:1989
5. Huyskens FL, Huyskens PL, Persoons AP (1998) J Chem Phys 108:8161
6. Turi L, Dannenberg JJ (1996) J Phys Chem 100:9638
7. Szostak MM, Kozankiewicz B, Wojcik G, Lipinski J (1998) J Chem Soc Faraday Trans 94:3241
8. Hurst M, Munn RW (1989) Special publication, Royal Society of Chemistry (Org Mater non-linear Opt) 69:3
9. Hutter J, Wagniere G (1988) J Mol Struct 175:159
10. Dannenberg JJ (1991) ACS Symp Ser (Mater Nonlinear Opt) 455:457
11. Wesch A, Dannenberger O, Wöll C, Wolff JJ, Buck M (1996) Langmuir 12:5330
12. Schmid ED, Moschallski M, Peticolas WL (1986) J Phys Chem 90:2340
13. Kumar K, Carey PR (1975) J Phys Chem 63:3697
14. Schmidt PH, Plieth WJ (1986) J Electroanal Chem 201:163
15. Holze R, Surface and interface analysis: an electrochemists toolbox, Springer, Berlin Heidelberg New York, in preparation
16. Holze R (1991) Electrochim Acta 36:1523
17. Gao P, Weaver MJ (1985) J Phys Chem 89:5040
18. Li YS, Lin X, Cao YH (1999) Vib Spectrosc 20:95
19. Li Y-S, Vo-Dinh T, Stokes DL, Wang Y (1992) Appl Spectrosc 46:1354

20. Hu J, Zhao B, Xu W, Fan Y, Li B, Ozaki Y (2002) J Phys Chem B 106:6500
21. Hu J, Zhao B, Xu W, Fan Y, Li B, Ozaki Y (2002) Langmuir 18:6839
22. Roth I, Jbarah AA, Spange S, Holze R, work in progress
23. Astle MJ, McConnell WV (1943) J Am Chem Soc 65:35
24. Ravichandran C, Vasudevan D, Anantharaman PN (1992) J Appl Electrochem 22:1192
25. Jagganathan E, Mohamed M, Ahmed KAB, Anantharaman PN (1988) J Electrochem Soc India 37:65
26. Jagannathan E, Chellammal S, Tirunavukkarasu P, Anantharaman PN (1990) Trans SAEST 25:25
27. Holze R (1988) Surf Sci 202:L612
28. Holze R (1990) Electrochim Acta 35:1037
29. Karpiński ZJ, Kublik Z (1986) Pol J Chem 68:269
30. Testa AC, Reinmuth WH (1961) J Am Chem Soc 83:784
31. Stradins J, Kravis I (1975) J Electroanal Chem 65:635
32. Bencheikh-Sayarh S, Pouillen P, Martre A-M, Martinet P (1983) Electrochim Acta 28:627
33. Bencheikh-Sayarh S, Cheminat B, Mousset G, Pouillen P (1984) Electrochim Acta 29:1225
34. Mohammad M, Khan AY, Afzal M, Niza A, Ahmed R (1974) Aust J Chem 27:2495
35. Geske DH, Ragle JI, Bambenek MA, Balch AI (1964) J Am Chem Soc 86:987
36. Allendoerfer RD, Rieger PH (1966) J Am Chem Soc 88:3711
37. Runner ME (1952) J Am Chem Soc 74:3567
38. Shreve OD, Markham EC (1949) J Am Chem Soc 71:2993
39. Parkash R, Kalla RK, Verma RS (1976) Proc Indian Acad Sci 84A:64
40. Carastoian AI, Banica FG, Moraru M (1993) Rev Roum Chim 38:287; Carastoian AI, Banica FG, Moraru M (1993) 38:615
41. Tomat R (1970) Chimica e L'Industria 52:438
42. Ana MAS, Chadwick I, Gonzalez G (1982) Bol Soc Chil Quim 27:244
43. Ana MAS, Chadwick I, Gonzalez G (1985) J Chem Soc Perkin Trans II 1755
44. Wawzonek S, Mclntire TW (1967) J Electrochem Soc 114:1025
45. Shenglong W, Fosong W, Xiaohui G (1986) Synth Met 16:99
46. Heineman WR, Wieck HJ, Yacynych AM (1980) Anal Chem 52:345
47. Malitesta C, Palmizano F, Torsi L, Zambonin PG (1990) Anal Chem 62:2735
48. Ye B-X, Zhang W-M, Zhou X-Y (1997) Chin J Chem 15:343
49. Xu J, Sun X, Liu B, Xu F (2001) Anal Sci 17:i1363
50. Piette LH, Ludwig P, Adams RN (1962) Anal Chem 34:916
51. Kitani A, So Y-H, Miller LL (1981) J Am Chem Soc 103:7636
52. Kitani A, Miller LL (1981) J Am Chem Soc 103:3595
53. Ravichandran K, Baldwin RP (1983) Anal Chem 55:1586
54. Duca A, Bejan D (1991) Rev Roum Chim 36:439
55. Stočesová D (1949) Collect Czech Chem Commun 14:615
56. Yang L, Guang-Zhi X, Jing-Gui S, Jin-Liang G, You-Qi T (1989) Acta Chim Sin (Eng Ed) 4:365
57. Genies EM, Lapkowski M (1987) J Electroanal Chem 236:189
58. Bacon J, Adams RN (1968) J Am Chem Soc 90:6596
59. Roy BC, Gupta MD, Ray JK (1995) Macromolecules 28:1727
60. Koval'chuk EP, Whittingham S, Skolozdra OM, Zavalij PY, Zavaliy IY, Reshetnyak OV, Seledets M (2001) Mater Chem Phys 69:154; Koval'chuk EP, Whittingham S, Skolozdra OM, Zavalij PY, Zavaliy IY, Reshetnyak OV, Blazejowski J (2001) Mater Chem Phys 70:38
61. Varsányi G (1974) Assignments for vibrational spectra of seven hundred benzene derivatives. Adam Hilger, London
62. Dollish FR, Fateley WG, Bentley FF (1974) Characteristic Raman frequencies of organic compounds. Wiley, New York
63. Muniz-Miranda M (1997) J Raman Spectrosc 28:205
64. Gao X, Davies JP, Weaver MJ (1990) J Phys Chem 94:6858
65. Tanaka T, Nakajima A, Watanabe A, Ohno T, Ozaki Y (2003) J Mol Struct 661/662:437
66. Holze R (1987) Electrochim Acta 32:1527
67. Holze R (1988) J Electroanal Chem 250:143
68. Vaschetto ME, Retamal BA, Monkman AP (1999) J Mol Struct 468:209
69. Szostak MM (1979) J Raman Spectrosc 8:43
70. Boggetti H, Anunziata JD, Cattana R, Silber JJ (1994) Spectrochim Acta, 50A:719